Online Battery SOH Prediction under lntra-Cycle Variation of Discharge Current and Non-Standard Charging and Discharging Practices

Areum Kim[1] and Sukhan Lee[2*]

[1,2] *Sungkyunkwan University, Suwon, Gyeonggi-do, 16419, Republic of Korea*
aroma1532@skku.edu
lsh1@skku.edu

ABSTRACT

Online SOH prediction of a battery is essential for battery management and safety in real-world applications. Despite the many approaches proposed to date, most conventional approaches to online SOH prediction neither incorporate intra-cycle variation of discharge currents nor consider non-standard charging and discharging practices along cycles. However, it is crucial for real-world applicability to have online SOH prediction effective under load current variations and non-standard practices. In this paper, we present an approach to online SOH prediction with our emphasis on non-standard charging and discharging practices as well as intra-cycle load current variations in prediction. To this end, first, we represent a cyclic history of terminal voltages and currents by a sequence of four physical indicators of SOH: the total charge, the voltage-time entropy and the average and standard deviation of varying load current. A sequence of SOH indicators is then input to an LSTM stack for online SOH prediction. Notably, to deal with non-standard practices, we identify the minimum voltage ranges that non-standard practices should cover in order to predict SOH with sufficient accuracy. Furthermore, we convert the non-standard SOH to the equivalent standard indicators by a regression network so that the complexity in implementation is radically reduced. The results indicate that the proposed approach can provide accurate online SOH prediction even under randomly varying discharging currents and non-standard practices with RMSE errors of about 0.5% as well as R^2 of about 95%.

1. INTRODUCTION

Lithium-ion batteries are promising as energy storage devices for electrified vehicles and devices because of their high energy density, low self-discharge rate and long lifespan compared to other battery types. However, as the batteries age along the repeated charging and discharging cycles, their maximum usable capacity is gradually degraded. Moreover, the batteries degraded below a certain capacity can be deteriorated faster till they become inoperable or fallen, possibly, into a catastrophic failure. State of Health (SOH) is an indicator of battery's aging state, which represents a percentile ratio of the current battery capacity with respect to the nominal capacity specified by the manufacturer. When SOH of a battery drops down to a certain level, say 80%, it indicates the time to replace the battery for operability and safety. In this sense, online SOH estimation of batteries is important not only for effective battery management but also for safe use of batteries by avoiding such possible hazards as thermal runaway and fire. However, the accurate estimation of battery SOH online is difficult due to the complexity involved in the electrochemical behavior of batteries. Although measuring the battery electrochemical impedance with dedicated devices as well as the discharge capacity with standard load currents can provide a high precision of SOH estimates, they are not applicable to online applications. The many approaches to online SOH estimation to data are categorized into the model-driven approach and the data-driven approach. Model-driven approaches are based on clear physical groundings in implementation. However, their performance depends on the accuracy of the model used under the trade-off with the complexity in processing. On the other hand, the data-driven approaches can be simpler in implementation, while taking advantage of the recent advancement in deep learning technologies. However, their performance is limited by the amount and quality of the ground truth data available.

1.1. Related Work

Currently, the methods proposed for estimating battery SOH can generally be grouped into three categories: the direct measurement method, the model-based method, the data-driven method. The direct measurement method is a method of estimating SOH based mainly on the terminal voltage, current and impedance of the battery. Representatively, there are coulomb-counting method, OCV method and Impedance method and This method has relatively low computational complexity for SOH estimation. However, the coulomb-counting method, which estimate SOH by integrating currents, has a problem that the accuracy is low due to the accumulation of sensor noise in the process of integrating currents. Moreover, the OCV method and the internal impedance method, which estimate SOH through the relationship between OCV or internal resistance value and SOH, are difficult to estimate online SOH because must be kept in an idle state for measuring OCV and internal resistance value.

The model-based method defines a model through the equivalent circuit of the battery, and through this, explains the state change during battery operation and estimates the SOH. In this regard, Andre et al. (2013) introduced a method of predicting SOH using the Extended Kalman filter and Support Vector Regression together, and it shows that SOH prediction can be made by aging even if charging and discharging in different ways for each cycle in addition, Burgos et al. (2016) approximates the probability density function of the maximum available power of a battery using a particle filter-based nonlinear dynamic model. The model base method can estimate SOH online, unlike direct measurement method, by connecting the battery signal measured in real time with SOH through electrochemical model. However, the model parameter and state equation should be redefined depending on the battery used, and the values of some parameters can change over time, so these factors increase the error.

The data-driven method is a method of estimating SOH by training machine learning models such as neural networks and SVMs (Support Vector Machines) with battery data obtained through actual measurement. Lin et al. (2012) introduced a method of predicting SOH using a Probabilistic Neural Network (PNN), but this has the disadvantage of ensuring accuracy when there are enough training samples. Zhou et al. (2020) proposes a model that predicts SOH through the Temporal Convolution Network using data provided by Center for Advanced Life Cycle Engineering (CALCE) of Maryland University and provides accuracy of RMSE 0.011.

Especially, since the characteristics of the battery for SOH estimation have time-series characteristics, recurrent neural networks such as Long Short-Term Memory Model (LSTM) and Gated Recurrent Units (GRU) are mainly used for SOH estimation to reflect these characteristics. Ungurean et al. (2020) proposes a method to estimate SOH using GRU model with input of State of Charge (SOC) sequence data for each battery cycle and argues that the calculation can be reduced by using GRU model. However, this method needs to additionally design a battery model according to the method of predicting SOC in real time, and external factors need to be considered. Besides that, Wu et al. (2020) proposes a method of estimating SOH using LSTM model using the charging time data and the IC curve data as input vectors. This data-driven method estimates SOH using data collected under limited conditions. However, this method may be difficult to estimate accurately in real situations where the discharge current changes or the charge/discharge is non-standard.

1.2. PROBLEM FORMULATION AND PROPOSED APPROACH

Conventionally, deep learning-based approaches to battery SOH estimation using discharging characteristics have to rely on a small number of publicly accessible datasets collected with a constant discharging current at individual cycles. However, for real-world applications of battery SOH estimation, in which battery payload varies constantly in time and so does discharging current, SOH estimation should take into consideration the effect of inter- and intra-cycle variations of discharging current on SOH estimation. Note that SOH can also be estimated based on battery charging characteristics, instead of discharging characteristics, for which constant charging currents are in use. Although the SOH estimation using charging characteristics alleviates the issues involved in current variations, the performance of charging-based SOH estimation needs to be compared with that of the discharging-based SOH estimation prior to positioning the two approaches in real-world applicability. This leads to the necessity of investigating the following problems: 1) how to achieve accurate SOH estimation based on discharging characteristics under inter- and intra-cycle current variations and 2) how accurate discharging-based SOH estimation could be, in comparison with that of charging-based, if taking inter- and intra-cycle current variations into consideration.

Another issue to consider for real-world applicability is partial charging and discharging. Note that no full discharging and charging is guaranteed at every charging and discharging cycle. Unlike conventional approaches to SOH estimation that assume full charging and discharging at individual cycles, in reality, partial charging and discharging may well take place from cycle to cycle. Therefore, we need to be able to accurately estimate SOH even under the presence of partial charging and discharging cycles.

To address the problems associated with load current, first, we investigate how current variations affect SOH estimation by changing the voltage drop profile and the total amount of charges charged and discharged in a cycle. As the feature

representing voltage drop profile, we propose entropy of the time- vs. voltage- interval histogram or time-voltage distribution of a cycle. More specifically, we investigate the effect of discharging currents, including inter- and intra-cycle current variations, on the correlation between SOH and the time-voltage distribution entropy of a cycle as well as between SOH and the total amount of charges expended in a cycle. Then, we supplement the time-voltage distribution entropy and the total amount of charges in a cycle by adding the current standard deviation of a cycle as a means of compensating for the effect of current variations on SOH estimation. These features representing both the voltage and current profiles of a cycle are then input to an LSTM stack designed for SOH estimation to obtain accurate SOH estimation under current variations. On the other hand, to deal with the issues associated with partial charging and discharging, we investigate the effect of partial charging and discharging on SOH estimation and derive the critical ranges of charging and discharging voltages that should be included in SOH estimation to ensure the desired estimation accuracy.

2. ONLINE PREDICTION OF BATTERY SOH BASED ON CHARGING AND DISCHARGING PROFILES

Online SOH prediction of rechargeable batteries can be done based either on charging cycles or on discharging cycles. Online prediction based on charging cycles is simpler in implementation due to the constant current used in standard charging practices. No extra consideration of the effect of load current variations on SOH prediction is necessary. However, as far as the prediction performance is concerned, the discharging cycle-based prediction often provides better accuracy than the charging-based. Here, we present battery SOH prediction based on both charging and discharging cycles. Instead, our emphasis is given to how to handle non-standard charging and discharging practices as well as load current variations in discharging-based SOH prediction. By non-standard charging and discharging practices, we mean that charging or discharging is done by less than full charging or discharging between the lower and upper cut-off voltages: for instance, 2.7V and 4.2V for lower and upper cut-off voltages for the dataset we used in our experiments.

2.1. Charging Based Online SOH Prediction under Non-Standard Practices

As physical indicators of SOH degradation associated with charging, we consider the total amount of charges, Q, charged under the constant current and the voltage rise profile during charging at a particular cycle p. In particular, here, the voltage rise profile is represented as the voltage-time entropy, VE. VE is defined based on the probability distribution, $p(v_i)$, $i = 1, \dots, M$, of the time intervals associated with the voltage ranges, v_i, representing M constant voltage drops. The constant voltage drops are obtained by equally dividing the total range of voltage rise by M (e.g., $M = 17$ in our experiment). Then, VE is computed from $p(v_i)$, $i = 1, \dots, M$, by

$$VE = -\sum_{i=1}^{M} p(v_i) \log_{10} p(v_i) \quad (1)$$

As SOH is degraded due to battery aging, the voltage-time entropy, VE, increases while the total charge charged, Q, decreases with a clear correlation between SOH and VE and between SOH and Q.

Under the non-standard charging practices, batteries may be neither fully discharged prior to charging nor fully charged prior to discharging. Under this circumstance, the total charge charged and the voltage-time entropy vary according to the ranges of charging voltage that the non-standard charging practice imposes. This makes SOH prediction under non-standard practices difficult. Here, we investigate existence of the minimum voltage ranges in charging that are required for SOH prediction under non-standard charging practices. In Section 5, we show that such minimum voltage ranges exist such that we can predict SOH with sufficient accuracy under non-standard practices as long as charging covers the minimum ranges.

2.2. Discharging Based Online SOH Prediction under Non-Standard Practices and Payload Variations

For discharging-based SOH prediction, we consider not only the total charge, Q, discharged and the voltage-time entropy, VE, associated with the voltage fall during discharging, representing the same indicators used for charging-based SOH prediction. But also, we consider the inter- and intra-cycle variations of discharging currents under varying payloads that may affect the rate of SOH degradation. To this end, we include the average and standard deviation of discharging current as physical indicators of SOH in addition to Q and VE. This differs from conventional approaches to SOH prediction in which discharging currents are assumed constant within a cycle, if not the entire cycles. When intra-cycle discharging currents vary due to payload variations, the corresponding voltage drop profiles also vary, affecting the associated voltage-time entropies. Since it may be desired to have VE invariant to inter-cycle and intra-cycle current variations as a physical indicator of SOH, we propose to define a canonical form of discharging voltage profiles independent of current variations. To this end, we propose that, at cycle p, the terminal voltage, $V_T^p(t)$, be transformed into that of the open-circuit voltage (OCV), $V_o^p(t)$, by compensating the voltage drop due to the battery internal resistance, R_i^p, such that VE is obtained based on $V_o^p(t)$, :

$$V_o^p(t) = V_T^p(t) + R_i^p I^p(t) \quad (2)$$

where $I^p(t)$ represents the terminal current at cycle p. Although OCV has a nonlinear characteristic, in this case, it is valid in the limited stoichiometry range because it considers a very short time interval. The internal resistance,

R_i^p, which varies along cycle, p, is known to satisfy the following equation:

$$R_i^p = aSOH^p + b \quad (3)$$

where a = -0.5349 and b = 0.7684. Note that these coefficient values are obtained based on the CALCE Dataset by calculating R_i at each cycle with the given SOH. Since SOH^p is unknown at cycle p, we may use R_i^{p-1} instead of R_i^p as an approximation. Now, with the compensated discharge voltages, $V_o^p(t)$, VE associated with the voltage drop profile of a discharging cycle can be defined exactly same as that of the voltage rise profile of a charging cycle. Same as the case of charging, a clear correlation exists between VE and SOH and between Q and SOH in the case of discharging.

However, unlike the charging cycles based on the constant charging current, the intra-cycle as well as inter-cycle variations of load currents in discharging cycles are expected to influence battery aging or SOH degradation by themselves. Therefore, we consider it necessary to include the variation of discharging current as a physical indicator for SOH prediction. To this end, here, we introduce the average, I, and standard deviation, SD, of the discharging current of a particular cycle as additional physical indices for SOH prediction. In other words, in the case of discharging cycle-based SOH prediction under intra-cycle and inter-cycle current variations, we combine VE and Q with the average current, I, and the standard deviation, SD, at cycle p as physical indicators for SOH prediction. As a matter of fact, we experimentally verified that cyclic differences in the average current and standard deviation of load current result in differences in Q and VE profiles along the SOH degradation.

Same as the case of charging, we emphasize the SOH prediction under the non-standard discharging practices. That is, batteries may not be neither fully charged prior to discharging nor fully discharged prior to charging. In this case, the total charge discharged and the voltage-time entropy at cycle p vary according to the range of discharging voltages imposed by the non-standard discharging practice. However, as mentioned for the case of non-standard charging practices, there exist the minimum ranges of discharging voltages that ensure an effective SOH prediction as long as the non-standard practices cover the minimum voltage ranges. In Section 5, we present such minimum voltage ranges in details in terms of a 2D map of center voltage-voltage gap.

3. CONVERSION OF NON-STANDARD Q AND VE TO STANDARD Q AND VE

As shown in Section 5, there exist the minimum ranges of charging and discharging voltages that are required for the non-standard charging and discharging practices to cover to obtain sufficient accuracy in SOH prediction. However, the use of varying voltage ranges due to non-standard practices result in the variation in Q and VE due simply to the difference in voltage ranges on top of the variation due to SOH degradation. This makes the SOH prediction based on Q and VE highly complicated under non-standard practices, such that a huge amount of data is required for training the proposed deep prediction network. For instance, under non-standard practices, the input sequence to the proposed LSTM-based SOH prediction has to use a mixture of Qs and VEs obtained under the standard and non-standard practices. Besides, a variety of non-standard charging and discharging practices may correspond to a large number of different minimum voltage ranges, resulting in many different Qs and VEs to be used for SOH prediction. As a solution, we propose to convert the non-standard Q and VE from non-standard practices into the standard Q and VE from standard practices in such a way that they become equivalent in terms of SOH prediction. Then, the equivalent standard Qs and VEs converted from the non-standard Qs and VEs are used to define the input sequence for the SOH prediction network. Specifically, we propose a regression network to convert Q_n and VE_n values associated with a non-standard voltage range, (v_n^1, v_n^2), to the equivalent Q_s and VE_s values associated with the standard voltage range. The ground truth data to train the network are defined in such a way that (Q_s, VE_s) and $(v_n^1, v_n^2, Q_n, VE_n)$ correspond to the same SOH. Figure 1 illustrates the proposed conversion network composed of 5 fully connected layers for converting non-standard Q_n and VE_n to the equivalent standard Q_s and VE_s, where v_n^1 and v_n^2 are, respectively, the min and max of the voltage range. In addition, root-mean-square-error (RMSE) was used as the loss function for learning the proposed regression model, and Adam Optimizer was used as an optimizer for learning. Adam Optimizer is an optimizer that brings the advantages of the Momentum Optimizer and RMSProp Optimizer. It prevents the model from falling into the local minimum due to the Momentum Optimizer term and allows the parameters to be well learned by adjusting the learning rate due to the RMSProp term.

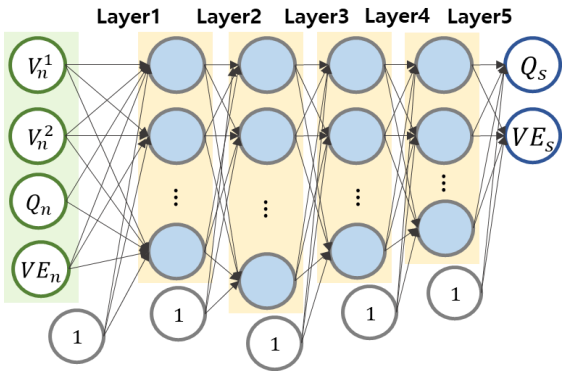

Figure 1. The proposed regression network designed to learn the conversion from non-standard $(V_n^1, V_n^2, Q_n, VE_n)$ to standard (Q_s, VE_s).

4. STACKED LSTM FOR SOH PREDICTION

For SOH prediction, we need to represent and learn the time-series relationship between SOH degradations and variations of battery physical indices, Q, VE, I and SD, along charging and discharging cycles. Here, we design a stacked LSTM with two LSTM layers and a fully connected layer to output predicted SOHs, as illustrated in Figure 2.

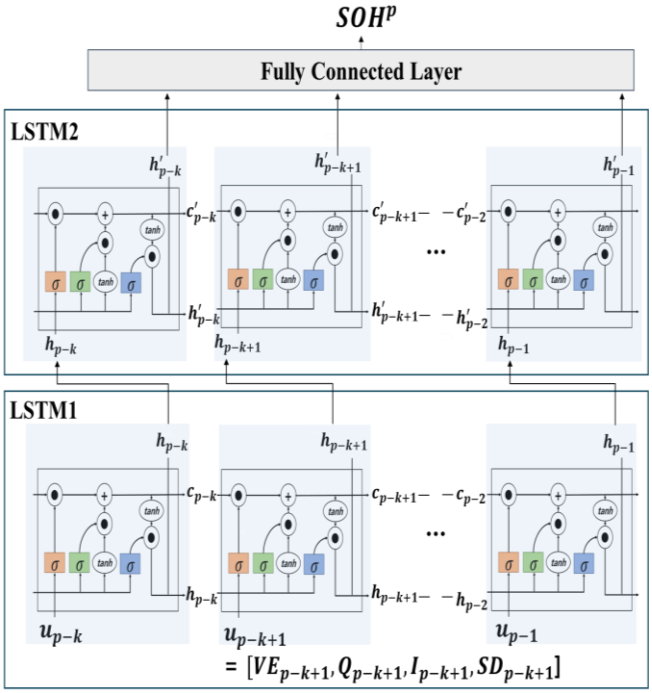

Figure 2. The proposed two-layer stacked LSTM with a fully connected output layer designed for SOH prediction at the p^{th} cycle.

The proposed stacked LSTM is intended to better extract temporal features embedded in an input sequence while taking advantage of LSTM for incorporating a longer-term temporal context. To predict the SOH at cycle p, the proposed stacked LSTM uses a sequence of k input vectors, $[u_{p-k}, u_{p-k+1}, \ldots, u_{p-1}]$, composed of battery physical index vectors, u_{p-j}, j=1, …, k, at the past k cycles. u_{p-j} at cycle p–j is expressed as $[VE_{p-j}, Q_{p-j}, I_{p-j}, SD_{p-j}]$, where $VE_{p-j}, Q_{p-j}, I_{p-j}$ and SD_{p-j} represent, respectively, the voltage-time entropy, the total charge, the average current and the standard deviation of the current at cycle $p-j$. Note that, in the case of charging cycle based SOH prediction, we assume constant current in charging such that SD_{p-j} becomes null. LSTM units in the first layer are governed by the following typical LSTM formula expressed for cycle $p-j$:

$$f_{p-j} = \sigma\left(W_f \cdot \left[h_{p-1-\mathrm{j}}, x_{p-j}\right] + b_f\right) \quad (4)$$

$$i_{p-j} = \sigma\left(W_i \cdot \left[h_{p-1-\mathrm{j}}, x_{p-j}\right] + b_i\right) \quad (5)$$

$$a_{p-j} = tanh\left(W_c \cdot \left[h_{p-1-\mathrm{j}}, x_{p-j}\right] + b_c\right) \quad (6)$$

$$C_{p-j} = f_p * C_{p-1-\mathrm{j}} + i_{p-j} * a_{p-j} \quad (7)$$

$$o_{p-j} = \sigma\left(W_o \cdot \left[h_{p-1-\mathrm{j}}, x_{p-j}\right] + b_o\right) \quad (8)$$

$$h_{p-j} = o_{p-j} * tanh\left(C_{p-j}\right) \quad (9)$$

where C_{p-j}, h_{p-j}, $\mathrm{f_{p-j}}$, i_{p-j} and o_{p-j} represent, respectively, the state, the output, the forget gate, the input gate and the output gate for cycle $p-j$. For the second layer LSTMs, we simply replace u_{p-j} of Eq. (9) by h_{p-j}. The fully connected layer receives all the outputs from the second LSTM Layer and use them as its input to output the predicted SOH at cycle p.

In the process of learning the model, to prevent the model from overfitting, the dropout method was used at the connection part of the layer. At this time, the dropout probability was set to 0.3. Adam Optimizer was used as an optimizer for learning. Moreover, the charge expended while the battery is discharged from the upper cut-off voltage of 4.2V to the lower cut-off voltage of 2.7V is defined as the SOH of the cycle and used as the ground truth SOH.

5. EXPERIMENTAL RESULT

In order to evaluate the performance associated with the proposed SOH prediction, we used the, publicly available, CALCE dataset provided by Maryland University as well as the dataset we collected based on a battery testing equipment using actual batteries. The CALCE dataset is based on a 1.1Ah lithium-ion battery. In particular, we used the CS2 family of dataset in the CALCE, which collects data by repeating standard full charge and full discharge, and a constant charge current of 0.55A was used for charging. On the other hand, in the case of discharge, various static discharge currents of 0.11A, 0.22A, 0.55A, 1.1A, 1.65A, 2.2A are used for data collection. For the data set collected, a 3.25Ah lithium-ion battery INR18650 was used. We collected total three datasets by repeating charging and discharging cycles with the constant charging current of 1.6A and 3.2A but with the randomly varying discharging currents in time within a cycle, where their average and standard deviation pairs are (1.4, 0.46), (1.6, 0.92) and (2.2, 1.02).

5.1. SOH Prediction under Inter- and Intra-Cycle Variations of Discharging Currents

First, we evaluated the performance of the proposed SOH prediction approach based on the four indices: voltage-time entropy, VE, total charge, Q, average current and standard deviation, I and SD, respectively. The performance in SOH prediction is compared between charging and discharging cycles as well as between with and without inter- and intra-cycle variations of discharging currents.

We implemented the proposed LSTM stack described in Section 4. We set the length of input sequence, k, as 20, while

normalizing the four indices forming an input vector in such a way that each index has a value between 0 and 1. To prevent training from overfitting, we applied a dropout strategy to connections between the LSTM stack and the fully connected layer with the dropout probability of 0.3. Besides, Adam optimizer is adopted in training to avoid falling into local minima.

To evaluate the performance of SOH prediction, we adopted the root-mean-square-error (RMSE) and the goodness-of-fit measure R^2, as shown in the following equations:

$$RMSE = \sqrt{\frac{1}{m}\sum_{i=1}^{m}(y_i - \hat{y}_i)^2} \quad (10)$$

$$R^2 = 1 - \sum_{i=1}^{m}(y_i - \hat{y}_i)^2 / \sum_{i=1}^{m}(y_i - \bar{y}_i)^2 \quad (11)$$

where y_i and $\hat{y}_i$ represent, respectively, the ground truth and the predicted SOHs at the i^{th} cycle and $\bar{y}$ the average of the ground truth SOHs under prediction. R^2 is introduced here to compensate for RMSE applied to a small scale of data in which low RMSE does not always mean good performance.

Table 1 summarizes performance of the proposed SOH prediction based on charging and discharging cycles when CALCE datasets are used for evaluation. In the table, prediction accuracies are evaluated using three types of datasets in CS2 family: Type 1 with two datasets, Type 2 with four datasets and Type 3 with one dataset. Note that the charging data collected for the chosen three types of datasets are based on standard current/voltage protocol with the constant charging current of 0.55A each cycle. On the other hand, the discharging data collected for Type 1 and Type 2 datasets are based on the constant discharging current of 0.55A and 1.1A, respectively, while the discharging data collected for Type 3 dataset are based on alternating constant currents of 0.11, 0.22, 0.55, 1.1, 1.65 and 2.2A along cycles. Among them, the total number of cycles for Type 1 data used as a test is 809, and the total number of cycles for Type 2 data is 919. Furthermore, the Type 3 dataset consists of 333 cycles for each discharge current.

In this table, test cases are divided into three cases as follow: Case 1, "Constant Current"; Case 2, "Varying Inter-Cycle Current"; Case3 "Constant Current + Varying Inter-Cycle Current". Case 1 is the result made through Type 1 and Type 2 dataset, and a pair of data from each type dataset was used for testing and the rest of the dataset was used for training. On the other hand, under Case 2, we used Type 3 dataset for evaluating SOH prediction in the case of constant intra-cycle but varying inter-cycle discharging currents. Since Type 3 dataset is the only dataset available for this testing, we randomly selected 60% and 40% of data, respectively, for training and testing. Case 3 is the result of integrating and verifying the training data and test data used above.

Table 1 indicates that the proposed SOH prediction can provide high prediction accuracy under constant currents and varying inter-cycle currents for charging and discharging based SOH predictions. Specifically, the proposed stacked LSTM with total charge, voltage-time entropy and average current as its input could achieve RMSE of less than 0.027 or R^2 of higher than 0.98 in prediction, at least, when constant currents are used within a cycle regardless of inter-cycle current variations, which is commensurate to the state-of-the-art performance in SOH prediction. Notably, the proposed SOH prediction is shown working stably, with sufficient generalization power, under various training-testing dataset configurations in different current modes, including the varying inter-cycle current mode.

Table 1. Performance of the proposed SOH prediction evaluated based on CALCE datasets.

Test case	Training Data	Testing Data	Charging Cycles		Discharging Cycles	
			RMSE	R^2	RMSE	R^2
Constant Current	Type 1 + Type 2	0.55A	0.06063	0.95565	0.02659	0.99213
		1.1A	0.01065	0.99739	0.00779	0.99855
Varying Inter-Cycle Current	Type 3 (60%)	Type 3 (40%)	0.00566	0.99285	0.00805	0.99039
Constant Current + Varying Inter-Cycle Current	Type 1+ Type 2+ Type 3 (60%)	0.55A	0.05211	0.95767	0.02267	0.98707
		1.1A	0.01394	0.99604	0.00865	0.99819
		Type 3 (40%)	0.00596	0.98810	0.00739	0.99147

Table 2 summarizes the SOH prediction performance when using only VE, Q, and current average as inputs and when using current standard deviation together with the proposed model when applied to a dataset collected with randomly varying discharging currents within a cycle. Three datasets, Random Current A, B and C, are collected for experiment by using INR18650 lithium-ion battery by fixing the charging current constant at 1.6A for entire cycles, but by randomly varying the discharging current within individual cycles with their average and standard deviation as (1.4A, 0.46) for Random Current A, (2.2A, 1.02) for Random Current B and (1.6A, 0.92) for Random Current C. Random Current A, B and C datasets consist of 698, 768 and 741 cycles, respectively.

In Table 2, test cases are divided into three cases as follow: Case 1, "1 Random Current (60%) and 1 Random Current (40%)"; Case 2, "3 Random Current (60%) and 1 Random Current (40%)"; Case3 "2 Random Current and 1 Random Current". Case 1 under the respective Training and Testing Data imply that 60% of data are randomly selected from individual dataset for training, while the rest 40% of data are

assigned for testing for discharging-cycle based SOH prediction. By the same token, case 2 under the respective Training and Testing Data imply that 60% of data are randomly selected from all three datasets for training, while the rest 40% of data from individual datasets are assigned for testing. On the other hand, case 3 under the respective Training and Testing Data implies that two datasets are used for training while the rest for testing for discharging-cycle based SOH prediction. Additionally, when the current standard deviation is used as an input, a value close to 0 is used for the current standard deviation because it is a constant current in the case of charging.

According to Table 2, in the case of charging, both when the current standard deviation is used as an input and when not, the RMSE is less than 0.008. However, in the case of discharge, when the current standard deviation is not used as an input, the maximum RMSE is 0.017, whereas when the current standard deviation is used together, the RMSE is greatly reduced to a maximum of 0.007. The result verifies that the proposed SOH prediction method based on the concatenation of average current and its standard deviation with voltage-time entropy and total charge to define the input unit vector for a stacked LSTM can effectively handle the complexity in SOH prediction due to varying discharging currents.

Table 2. Performance of the proposed SOH prediction evaluated based on collected datasets with random variations of discharging currents within a cycle.

Input Data	Training Data	Testing Data	Charging Cycles		Discharging Cycles	
			RMSE	R^2	RMSE	R^2
VE, Q, Current Average (3 input)	1 Random Current (60%)	1 Random Current (40%)	0.00521	0.96053	0.01016	0.91371
	3 Random Current (60%)	1 Random Current (40%)	0.00626	0.94107	0.00859	0.93829
	2 Random Current	1 Random Current	0.0068	0.95372	0.01762	0.86101
VE, Q, Current Average, Current Standard deviation (4 input)	1 Random Current (60%)	1 Random Current (40%)	0.00689	0.96028	0.00395	0.96029
	3 Random Current (60%)	1 Random Current (40%)	0.00794	0.94716	0.00685	0.96072
	2 Random Current	1 Random Current	0.00747	0.95993	0.00449	0.96322

Figure 3 is a graph expressing the estimation results of the proposed model and the ground truth SOH when used as testing data discharged for Case 3. In Figure 3, (a) is a case where discharge data is used as an input and (b) is a case where charging data is used as an input. Through this result, the estimated value of the proposed model reflects the ground truth SOH trend well and that SOH estimation is possible with high accuracy.

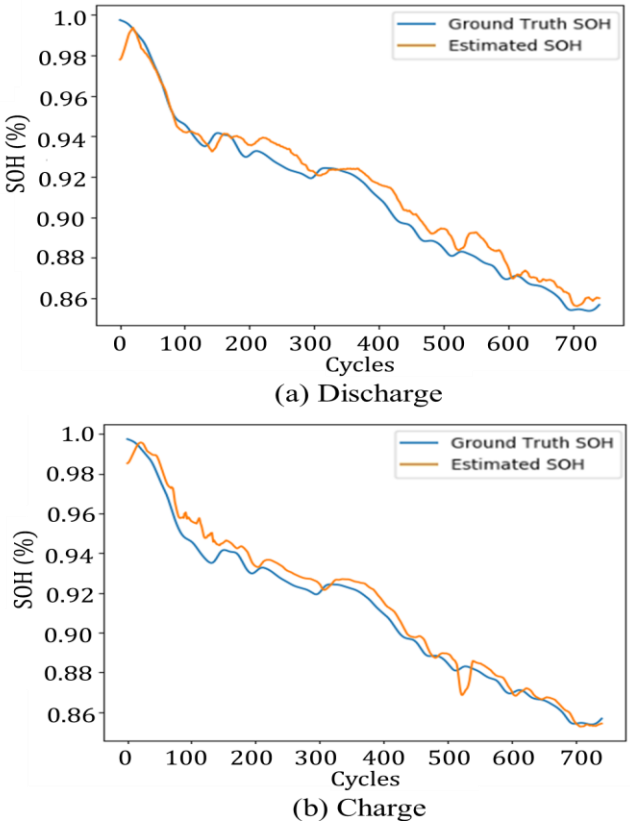

Figure 3. When the discharge current changes within 1 cycle, the result of estimating SOH using the total discharge data (a) and charge data (b).

5.2. Online SOH Prediction under Non-Standard Charging and Discharging Practices

For online SOH prediction, we need to take the non-standard practices in charging and discharging into consideration, besides the intra-cycle discharging current variations. In Section 2, we presented an approach for the proposed LSTM-based SOH prediction to deal with the indices from a mixture of standard and non-standard charging and discharging practices. To implement the proposed approach, first, we need to identify the minimum upper-lower cut-off ranges in charging and discharging voltages that are required for a sufficient accuracy in SOH prediction.

Here, we represent such a minimum upper-lower cut-off voltage range by using a 2D map with its two axes

representing, respectively, the center and the gap between the upper and the lower voltage range. This representation allows the voltage ranges effective for SOH prediction to be represented as the region in the 2D map, as illustrated in Figures 4. We constructed such 2D maps experimentally by using CALCE datasets, for which training and testing datasets were collected from all CS2 family of CALCE dataset. To have a high precision of 2D map, we divide the upper-lower cut-off voltage range between 3.0V and 4.1V by 0.1V with the gap resolutions of 0.3V, 0.5V and 0.7V in obtaining the R2 performance of the predicted SOHs for the ranges.

Figure 4 (a) represents the region (green) on the center-gap map inside which R^2 is 0.97 or higher for discharging-based SOH prediction. On the other hand, Figure 4 (b) represents the region (green) on the center-gap map inside which R^2 is 0.97 or higher for charging-based SOH prediction. The results were conducted through the CALCE dataset, and the R^2 for the test dataset was reflected by composing the training data and the test data in the same way as the test case 1 in Table I. That is, results for both aged and new battery cells are included. Figure 4 indicate that, in case of discharging-based SOH prediction, the center voltage between 3.7V and 3.9V with the gap more than 0.3V represent the critical requirement for R^2 to be higher than 0.98. On the other hand, in case of charging-based SOH prediction, the center voltage between 3.9V to 4.0V with the gap more than 0.4V are required. Figure 4 also indicate that discharging-based SOH prediction has a wider region on the center-gap map for effective SOH prediction than charging-based SOH prediction.

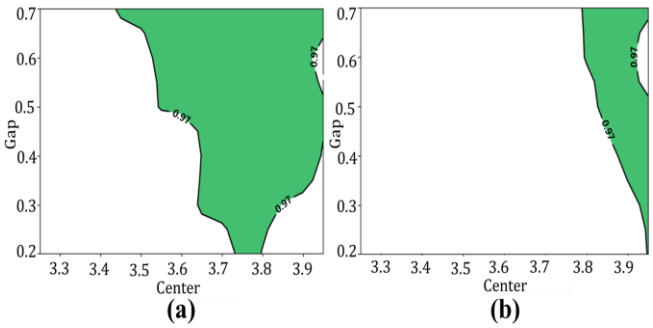

Figure 4. Region with high R^2 of (a) discharging voltage and (b) charging voltage.

Table 3 shows the results of equivalence transformation of Q and VE in the non-standard voltage range to Q and VE in the standard voltage range through the proposed regression network. In this case, Types 1 and 2 of the CS-2 family of CALCE datasets are used, and one dataset of each type was used as a test and the rest of the data was used for training. In order to evaluate the efficiency of the proposed equivalent conversion, experiments were conducted with and without the input data in the minimum voltage range derived above. First, the dataset was collected by fixing the gap of the voltage range to 0.7, 0.5, and 0.3 and changing the center. In this case, the minimum voltage range is not considered as shown in Figure 4. The second dataset is collected in such a way that the voltage ranges selected include the required minimum voltage ranges. In this case, the voltage range for charging consists of (4.2 - 3.5), (4.2 - 3.7), (4.1 - 3.6) and (4.1 - 3.8)V, and the voltage range for discharging consists of (4.2 - 3.7), (4.2 - 3.5), (4.1 - 3.4), (4.1 - 3.6), (3.9 - 3.2), (3.9 - 3.4) and (3.9 - 3.6)V. Note that, In both case, the data for which VE becomes null due to insufficient gap in the voltage range is removed.

Table 3. % RMSE error performance of the proposed regression network to transform from non-standard to standard VE and Q

Voltage Range	Testing Data	Charging Cycles % RMSE Error		Discharging Cycles % RMSE Error	
		VE	Q	VE	Q
Any ranges with a gap of 0.7	0.55A	0.73110	1.99248	1.11848	3.45743
	1.1A	0.74109	1.47223	1.51512	4.76091
Any ranges with a gap of 0.5	0.55A	1.30375	9.46749	1.14100	2.55281
	1.1A	1.12372	6.34241	1.52201	5.50048
Any ranges with a gap of 0.3	0.55A	1.76087	26.31565	1.60255	6.32801
	1.1A	1.39774	20.38615	2.345657	8.68956
Varying gap with the minimum ranges included	0.55A	1.38803	7.26720	2.13823	8.22401
	1.1A	1.13915	7.01399	1.73578	6.85647

According to Table 3, when the minimum range is not considered, the equivalent transformation error increases as the voltage gap decreases. In particular, in the case of charging, the error increases significantly as the gap changes, and when the gap is 0.3, the error of Q becomes up to 26%. On the other hand, when the minimum range is observed, equivalent transformation can be performed with VE less than 2% and Q less than 8% for both charging and discharging. That is, it is necessary for the equivalence transformation to observe the required minimum voltage ranges as shown in the worse performance of the charge with a fixed gap that more violates the minimum voltage range.

Finally, we evaluated the performance of SOH prediction in non-standard cases by applying a pre-trained equivalent transform to the stacked LSTM model for SOH prediction. Here, the 20 cycles used as input sequences for the stacked LSTM are divided into a case of application of non-standard practice and a case of using non-standard practice and standard practice together. When a non-standard practice is applied as an input sequence, the SOH prediction result is shown in Table 4, and the test case is divided into the case of using the voltage gap of 0.7, 0.5, 0.3v, the voltage gap between 0.3 and 0.7, and the case of using only the gap included in the minimum range. At this time, the data of the non-standard voltage range used to generate the input sequence is randomly selected from the test data set used for the evaluation of equivalent transformation. Additionally, as a model for SOH prediction, a model trained on constant current using the Type 1 and Type 2 datasets of CALCE presented above was used, and this result was compared with Table 1 showing the results for standard practice, and the change in error was additionally indicated.

Table 4. Performance of SOH prediction under non-standard charging and discharging practices.

Input Sequence	Testing Data	Charging Cycles		Discharging Cycles	
		RMSE	R^2	RMSE	R^2
Non-Standard data (Gap 0.7v)	0.55A	0.06494 (+0.0043)	0.95266 (-0.0030)	0.04742 (+0.0208)	0.97464 (-0.0175)
	1.1A	0.02907 (+0.0184)	0.98007 (-0.0173)	0.03417 (+0.0264)	0.97221 (-0.0263)
Non-Standard data (Gap 0.5v)	0.55A	0.09059 (+0.0300)	0.91986 (-0.0358)	0.02822 (+0.0016)	0.99137 (-0.0008)
	1.1A	0.03475 (+0.0241)	0.97162 (-0.0258)	0.03210 (+0.0243)	0.97543 (-0.0231)
Non-Standard data (Gap 0.3v)	0.55A	0.14555 (+0.0849)	0.76302 (-0.1926)	0.04336 (+0.0168)	0.97938 (-0.0128)
	1.1A	0.04083 (+0.0302)	0.96092 (-0.0365)	0.03874 (+0.0309)	0.96443 (-0.0341)
Non-Standard data (Gap 0.3~0.7v)	0.55A	0.07456 (+0.0139)	0.94336 (-0.0123)	0.03288 (+0.0063)	0.98863 (-0.0035)
	1.1A	0.03160 (+0.0210)	0.97649 (-0.0123)	0.02619 (+0.0184)	0.98353 (-0.0150)
Non-Standard data (Minimum ranges included)	0.55A	0.07468 (+0.0141)	0.94322 (-0.0124)	0.05170 (+0.0251)	0.96894 (-0.0232)
	1.1A	0.03489 (+0.0242)	0.97137 (-0.0260)	0.03042 (+0.0226)	0.97790 (-0.0207)

According to Table 4, if the minimum range is not considered when composing a sequence with non-standard data, the SOH prediction error increases as the voltage gap decreases, and this increase rate is larger in the case of charging. Moreover the SOH prediction result to compose the sequence considering the Minimum Range provides an RMSE error of less than 0.08 in the case of charging and less than 0.06 in the case of discharging, and in particular, the performance in case of charging is greatly improved. In other words, this indicates the need to observe with the minimum range when using non-standard practice data.

Table 5 shows the SOH prediction results for the mixed input of non-standard practices and standard practices. At this time, the experiment was conducted by dividing the ratio of non-standard practice and standard practice into 50%/50% and 30%/70%, respectively. For this result, the same model as the experiment for the above non-standard practice was used, and the results were compared with Table 1. As expected, the higher the ratio of non-standard practices for both charging and discharging, the greater the SOH prediction error. However, when predicting SOH through the proposed method, even when the ratio of non-standard practice is 50%, RMSE of less than 0.07 for charge and less than 0.05 for discharge is provided. This indicates that the SOH can be predicted almost similarly to the standard practice even in the case of a non-standard battery that does not fully discharge and charge the battery through the proposed method.

Table 5. SOH predictive performance under non-standard and standard charging and discharging practices.

Input Sequence	Testing Data	Charging Cycles		Discharging Cycles	
		RMSE	R^2	RMSE	R^2
Non-standard (50%) + Standard data (50%)	0.55A	0.06962 (+0.0090)	0.94859 (-0.0071)	0.04331 (+0.0167)	0.97943 (-0.0127)
	1.1A	0.03146 (+0.0208)	0.97669 (-0.0207)	0.02179 (+0.0140)	0.98853 (-0.0100)
Non-standard (30%) + Standard data (70%)	0.55A	0.06584 (+0.0052)	0.95194 (-0.0037)	0.03649 (+0.0099)	0.98593 (-0.0062)
	1.1A	0.02968 (+0.0190)	0.97923 (-0.0182)	0.99050 (+0.9827)	0.99131 (-0.0072)

6. DISCUSSION AND CONCLUSION

In this paper, we presented an approach to SOH prediction based on four physical SOH indicators, Q, VE, I and SD, associated with charging and discharging cycles, especially, with our emphasis on estimating SOH under non-standard charging and discharging practices as well as under intra-cycle and inter-cycle payload variations. We showed that the introduction of I and SD as SOH indicators is effective for predicting SOH under the variation of load current in

discharging cycles. In particular, in terms of dealing with non-standard practices, we provided the minimum voltage ranges that non-standard practices should cover to achieve SOH prediction with sufficient accuracy. Furthermore, we devised a method of converting the non-standard Q and VE to the equivalent standard Q and VE, thus avoiding excessive complexity in SOH prediction under non-standard practices. Since the proposed approach resorts to deep learning for relating a sequence of four SOH indicators to SOH as well as regressing the equivalent standard Q and VE from the non-standard Q and VE, the availability of a sufficient amount of ground truth data is important. We plan to incorporate a more variety of loading conditions and non-standard practices in SOH prediction for our future research.

ACKNOWLEDGEMENT

This work was supported, in part, by the e-Drive Train Platform Development Project, KETEP 20172010000420, of Korea Institute of Energy Technology Evaluation and Planning (KETEP), MOTIE, in part, by the Korea Health Technology R&D Project, Grant No. HW20C2077, of the Korea Health Industry Development Institute (KHIDI), MOHW, in part, by AI Graduate School Program, Grant No.2019-0-00421, and by ICT Consilience Program, IITP-2020-0-01821, of the Institute of Information and Communication Technology Planning Evaluation (IITP), sponsored by the Korean Ministry of Science and Information Technology (MSIT).

REFERENCES

Zhang, L., Hu, X., Wang, Z., Sun, F., Deng, J., & Dorrell, D. G. (2017) Multiobjective optimal sizing of hybrid energy storage system for electric vehicles. IEEE Transactions on Vehicular Technology 67.2, pp 1027-1035.

Zou, C., Zhang, L., Hu, X., Wang, Z., Wik, T., & Pecht, M. (2018) A review of fractional-order techniques applied to lithium-ion batteries, lead-acid batteries, and supercapacitors. Journal of Power Sources 390, pp. 286-296.

Tan, Yandan, and Guangcai Zhao. (2019) Transfer Learning with Long Short-Term Memory Network for State-of-Health Prediction of Lithium-ion Batteries. IEEE Transactions on Industrial Electronics 67.10, pp. 8723-8731.

Ng, K. S., Moo, C. S., Chen, Y. P., & Hsieh, Y. C. (2009) Enhanced coulomb counting method for estimating state-of-charge and state-of-health of lithium-ion batteries. Applied energy 86.9, pp, 1506-1511.

Weng, Caihao, Jing Sun, and Huei Peng. (2014) A unified open-circuit-voltage model of lithium-ion batteries for state-of-charge estimation and state-of-health monitoring. Journal of power Sources 258, pp. 228-237.

Li, S. E., Wang, B., Peng, H., & Hu, X. (2014) An electrochemistry-based impedance model for lithium-ion batteries. Journal of Power Sources 258, pp. 9-18.

Andre, D., Appel, C., Soczka-Guth, T., & Sauer, D. U. (2013) Advanced mathematical methods of SOC and SOH estimation for lithium-ion batteries. Journal of power sources 224, pp. 20-27.

Andre, D., Nuhic, A., Soczka-Guth, T., & Sauer, D. U. (2013) Comparative study of a structured neural network and an extended Kalman filter for state of health determination of lithium-ion batteries in hybrid electric vehicles." Engineering Applications of Artificial Intelligence 26.3, pp. 951-961.

Burgos-Mellado, C., Orchard, M. E., Kazerani, M., Cárdenas, R., & Sáez, D. (2016). Particle-filtering-based estimation of maximum available power state in Lithium-Ion batteries. Applied Energy, 161, 349-363

Hannan, M. A., Hoque, M. M., Hussain, A., Yusof, Y., & Ker, P. J. (2018) State-of-the-art and energy management system of lithium-ion batteries in electric vehicle applications: Issues and recommendations. Ieee Access 6, 19362-19378.

Hannan, M. A., Lipu, M. S. H., Hussain, A., Saad, M. H., & Ayob, A. (2018) Neural network approach for estimating state of charge of lithium-ion battery using backtracking search algorithm. Ieee Access 6, 10069-10079.

Li, X., Shu, X., Shen, J., Xiao, R., Yan, W., & Chen, Z. (2017) An on-board remaining useful life estimation algorithm for lithium-ion batteries of electric vehicles. Energies 10.5, 691.

Lin, H. T., Liang, T. J., & Chen, S. M. (2012). Estimation of battery state of health using probabilistic neural network. IEEE transactions on industrial informatics, 9(2), 679-685.

Zhou, D., Li, Z., Zhu, J., Zhang, H., & Hou, L. (2020) State of Health Monitoring and Remaining Useful Life Prediction of Lithium-Ion Batteries Based on Temporal Convolutional Network. IEEE Access 8, 53307-53320.

Ungurean, Lucian, Mihai V. Micea, and Gabriel Cârstoiu. (2020) Online state of health prediction method for lithium ‐ ion batteries, based on gated recurrent unit neural networks." International Journal of Energy Research.

Wu, Y., Xue, Q., Shen, J., Lei, Z., Chen, Z., & Liu, Y. (2020) State of Health Estimation for Lithium-Ion Batteries Based on Healthy Features and Long Short-Term Memory. IEEE Access 8, 28533-28547.

You, Gae-Won, Sangdo Park, and Dukjin Oh. (2017) Diagnosis of electric vehicle batteries using recurrent neural networks. IEEE Transactions on Industrial Electronics 64.6, 4885-4893.

Berecibar, M., Gandiaga, I., Villarreal, I., Omar, N., Van Mierlo, J., & Van den Bossche, P. (2016). Critical review of state of health estimation methods of Li-ion batteries for real applications. Renewable and Sustainable Energy Reviews, 56, 572-587.

Rivera-Barrera, J. P., Muñoz-Galeano, N., & Sarmiento-Maldonado, H. O. (2017). SoC estimation for lithium-

ion batteries: Review and future challenges. Electronics, 6(4), 102.

Eberle, U., & Von Helmolt, R. (2010). Sustainable transportation based on electric vehicle concepts: a brief overview. Energy & Environmental Science, 3(6), 689-699.

Kim, A., & Lee, S. (2021, January). Online State of Health Estimation of Batteries under Varying Discharging Current Based on a Long Short Term Memory. In 2021 15th International Conference on Ubiquitous Information Management and Communication (IMCOM) (pp. 1-6). IEEE.

Bak, T, & Lee, S. (2019, September). Accurate estimation of battery SOH and RUL based on a progressive lstm with a time compensated entropy index. In Annual Conference of the PHM Society (Vol. 11, No. 1, pp. 2012-2013).

BIOGRAPHIES

Areum Kim received her B.S degrees in Electronic and Electrical Engineering from Chung-ang University in 2015. From 2016 to 2019, she was the engineer at HUMAX Automotive. Her research interests are in the areas of PHM based on intelligent systems, and time series analysis with machine learning. She is currently a Master's student at Sungkyunkwan University.

Sukhan Lee This received the B.S. and M.S. degrees in electrical engineering from Seoul National University, South Korea, in 1972 and 1974, respectively, and the Ph.D. degree in electrical engineering from Purdue University, West Lafayette, IN, USA, in 1982. From 1983 to 1997, he was with the Department of Electrical Engineering and Computer Science, University of Southern California. From 1990 to 1997, he was with the Jet Propulsion Laboratory, California Institute of Technology. From 1998 to 2003, he was the Executive Vice President and the Chief Research Officer with the Samsung Advanced Institute of Technology. Since 2003, he has been a Professor of information and communication engineering with Sungkyunkwan University. His research interest in the areas of cognitive robotics, intelligent systems, deep learning, and micro/nano electro-mechanical systems. He is currently a Life Fellow of the Korea National Academy of Science and Technology.